

# LONGITUDINAL DIAGNOSTICS FOR SHORT ELECTRON BEAM BUNCHES\*

H. Loos<sup>†</sup>, SLAC, Menlo Park, CA 94025, USA

## Abstract

Single-pass free electron lasers require high peak currents from ultra-short electron bunches to reach saturation and an accurate measurement of bunch length and longitudinal bunch profile is necessary to control the bunch compression process from low to high beam energy. The various state-of-the-art diagnostics methods from ps to fs time scales using coherent radiation detection, RF deflection, and other techniques are presented.

## INTRODUCTION

The use of linear accelerators as drivers for free electron lasers (FEL) and the advent of single-pass (SASE) FELs has driven the development of a wide range of diagnostic techniques for measuring the length and longitudinal distribution of short and ultra-short electron bunches. For SASE FELs the radiation power and the length of the undulator needed to achieve saturation depend strongly on the charge density of the electron beam. In the case of X-ray FELs [1, 2, 3], this requires the accelerator to produce ultra-high brightness beams with micron size transverse normalized emittances and peak currents of several kA through several stages of magnetic bunch compression. Different longitudinal diagnostics are employed to measure the peak current and bunch profile along these stages.

The measurement techniques can be distinguished into different classes. Coherent methods detect the light emitted from the beam by some coherent radiation process (spectroscopic measurement), or directly measure the Coulomb field traveling with the beam (electro-optic). Phase space manipulation techniques map the time coordinate onto a transverse dimension and then use conventional transverse beam diagnostics (transverse deflector, rf zero-phasing). Further methods measure the profile or duration of an incoherent light pulse emitted by the bunch at wavelengths much shorter than the bunch length (streak camera, fluctuation technique) or modulate the electron beam at an optical wavelength and then generate a narrow bandwidth radiation pulse with the longitudinal profile of the beam mapped onto (optical replicator).

The operational needs for bunch length measurements to have fast acquisitions, to be used in feedback systems, to distinguish pulse to pulse changes and to be non-destructive or parasitically have resulted into developing many of the diagnostics into single-shot techniques and in the following the main discussion will emphasize them.

## PHASE-SPACE METHODS

A direct method to measure the length and structure of short electron bunches is the use of a phase-space transformation to map time onto a transverse coordinate. The measurement then relies on conventional transverse beam diagnostics to obtain the beam size or beam profile with screens or wire scanners. One method uses a longitudinal phase space transformation by setting one of the accelerating structures to the zero-crossing phase to map time onto energy and then measuring the energy distribution of the beam in a dipole spectrometer [4]. Although straightforward to implement, this method requires a dedicated diagnostics beam line and accelerator setup, and time-energy correlations in the phase-space require tomographic methods to get resolved [5]. A different method is to use a transverse deflecting cavity to map time directly onto a spatial coordinate.

### Transverse Deflecting Cavity

Originally developed at SLAC in the 1960s [6], the transverse deflector cavity has in recent years been used as a high resolution bunch length diagnostics at DESY [7] and at SLAC [8, 9, 10] in the range of bunch lengths from sub-millimeter to a few micrometer. The operating principle is shown in Fig. 1. An S-band traveling wave structure induces a vertical kick to the electron beam. At a screen downstream of the deflector with  $\Delta\psi = 90^\circ$  betatron phase advance this leads to a vertical offset of the beam. When the cavity is operated at either zero-crossing phase  $\phi = \pm 90^\circ$ , the bunch becomes tilted and the vertical beam size depends on the bunch length as

$$\sigma_y^2 = \sigma_{y,0}^2 + \beta_d \beta_s \sigma_z^2 \left( \frac{k_{\text{RF}} e V_0 \sin \Delta\psi \cos \phi}{E_s^2} \right)^2 \quad (1)$$

with  $E_s$  the beam energy at the screen and  $k_{\text{RF}}$  the RF angular wave number.

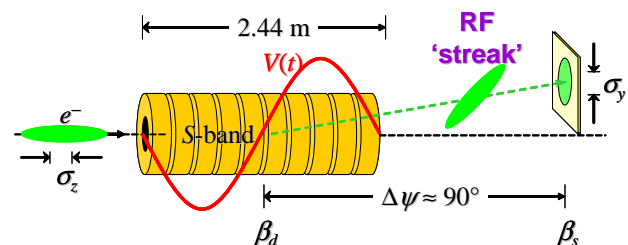


Figure 1: Principle of bunch length measurement using a transverse deflecting rf-cavity.

\* Work supported by US DOE contract DE-AC02-76SF00515.

<sup>†</sup> loos@slac.stanford.edu

At LCLS, two deflector cavities at 135 MeV and 4.7 GeV energy can operate at maximum deflection voltages  $V_0$  of 1 MV and 25 MV, respectively. The high energy cavity also has an upstream horizontal kicker magnet to measure the bunch length parasitically to normal operations at an off-axes screen. In order to maximize the streak effect and the temporal resolution, the beam size at the deflecting cavity needs to be as large as possible and the lattice phase advance to the screen optimized to be close to  $90^\circ$ . Fig. 2 shows OTR images of the beam in the LCLS injector with the deflector off and on at 1 MV.

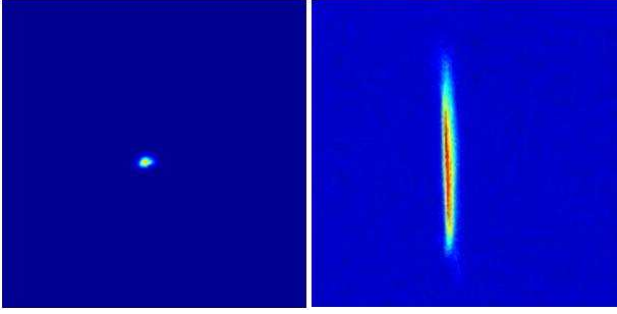


Figure 2: OTR beam images in the LCLS injector at 135 MeV for a  $800\ \mu\text{m}$  long bunch with the deflecting cavity off (left) and on at 1 MV (right). The vertical beam sizes are approximately  $60\ \mu\text{m}$  when off and  $60\ \mu\text{m}$  when on.

The time calibration of the beam size measurement is done by shifting the phase of the cavity by a few degrees and observe the corresponding shift in the centroid position of the beam on the screen. For the low energy deflector, a typical calibration ratio  $R_{35}$  is 1, i.e. 1 transverse mm per 1 longitudinal mm, which enables comfortable bunch length measurements well below  $100\ \mu\text{m}$ . The resolution limit can be estimated from Eq. 1 and the uncertainty in the beam size measurement to

$$\Delta\sigma_z = R_{35}\sigma_{y,0}\sqrt{2\frac{\Delta\sigma_{y,0}}{\sigma_{y,0}}}. \quad (2)$$

For the high energy deflector cavity, a calibration ratio of about 20 can be realized on a phosphor screen with an intrinsic beam size of  $200\ \mu\text{m}$  which gives a temporal resolution of  $1.5\ \mu\text{m}$  or 5 fs assuming a 1% accuracy for the beam size measurement. Fig. 3 shows the results for a 250 pC beam at nominal compression with  $8\ \mu\text{m}$  bunch length and in the extreme case of maximum compression with  $2\ \mu\text{m}$ . This measurement of an ultra-short bunch length is supported by Elegant simulations [10] shown in Fig. 4 which fit well the measured bunch length as a function of bunch compressor  $R_{56}$ .

Recent studies [11] indicate that at a very low charge of 20 pC the generation of sub-micron pulses becomes possible. Such bunch lengths can presently not be resolved, but the resolution limit of a few fs could be lowered by increasing the RF frequency from S-band to X-band [12].

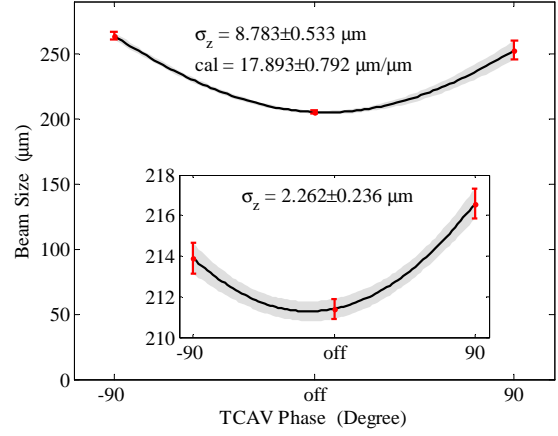


Figure 3: Transverse deflector bunch length measurement in the LCLS linac at 4.7 GeV after the second bunch compressor. The large figure shows the measurement at normal compression and the inset shows a measurement at maximum compression.

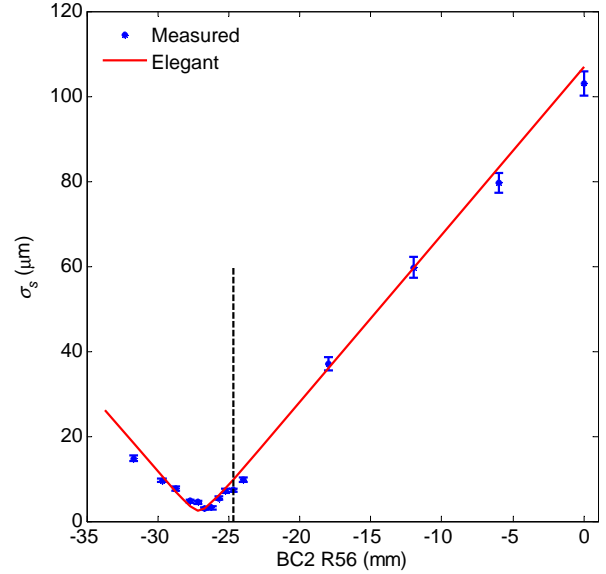


Figure 4: Bunch length measured in the LCLS linac at 4.7 GeV vs. compression in the second bunch compressor using a transverse cavity.

The transverse beam size measurement in the case of ultra-short bunches with lengths corresponding to visible or infrared wavelengths are severely impeded by coherent radiation effects [13] in the case of OTR screens and high energy measurements could only be done on a phosphor screen. The use of wire scanners and a beam based feedback for the deflector cavity phase is currently tested and alternatives to OTR screens are being studied.

## COHERENT METHODS

The coherent methods use the fact that the Coulomb field traveling with an electron bunch follows the temporal distribution of the bunch and this distribution can be maintained in a light field emitted by a coherent radiation process. The Coulomb or radiation field can then be measured directly with electro-optic methods, enabling a direct pulse shape determination. Spectral methods measure the spectral light intensity and the unknown phase information needs to be recovered, leaving ambiguity in the reconstructed pulse shape. In both methods, the measured electro-optic signal or autocorrelation trace from an interferometer is based on a convolution of the original longitudinal bunch distribution with the response function of the detection system. Hence the temporal resolution and usable bunch length range depend on the spectral bandwidth of the detection method and the quality of the bunch shape measurement relies on how well the response function can be determined.

### Spectroscopy

The observation of coherent radiation from ps and sub-ps long electron bunches [14] at mm wavelengths and in the far infrared has been utilized over the past two decades as a widely applied bunch length and bunch shape diagnostics. The measured radiation spectrum  $W(\omega)$  for  $N$  electrons depends on the Fourier transform of the charge distribution  $f(\omega)$  by

$$W(\omega) = W_0(\omega) \left( N + (N-1)N |f(\omega)|^2 \right) \quad (3)$$

with  $W_0(\omega)$  the emission spectrum of a single electron for the particular radiation process, e.g. coherent transition, edge, synchrotron, or any other coherent radiation process. The absolute square of  $f(\omega)$  is also called the bunch form factor  $F(\omega)$ . The radiation spectrum is usually measured with some sort of scanning interferometer and when  $W_0(\omega)$  is well known, the form factor and the bunch length can be determined. Using a Kramers-Kronig relation, the phase can also be retrieved in many cases and the pulse shape can be reconstructed with an inverse Fourier transform [15].

The usage of a scanning interferometer makes this method less suited for fast measurements, but the observation of coherent radiation over a certain bandwidth with a single detector can be used as a relative bunch length monitor for feedback systems and be calibrated against other absolute measurements. Such relative monitors have been implemented e.g. at DESY [16] using gratings to discriminate spectral regions or at SLAC [17] using transmission filters for that purpose. Fig. 5 shows the implementation for LCLS of a coherent edge radiation monitor.

The monitor design and bandwidth selection depends on the bunch length range. The expansion of the form factor for small wave numbers

$$F(k) = 1 - k^2 \sigma_z^2 + O(k^4) \quad (4)$$

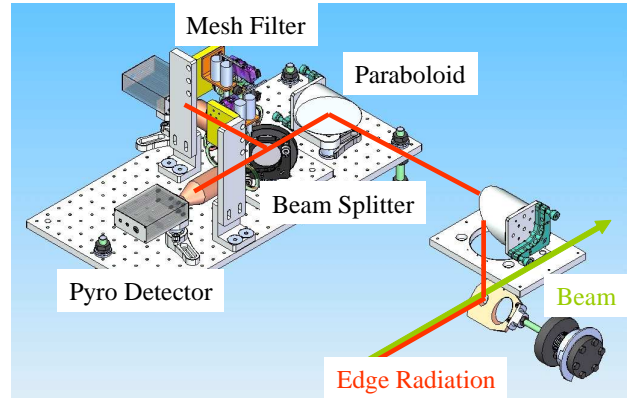


Figure 5: Schematic of the LCLS relative bunch length monitor using coherent edge radiation from an upstream bend magnet.

shows that the relevant spectral range to monitor bunch length is for wavelengths larger than  $2\pi\sigma_z$  where the form factor does not depend much on the specific shape of the charge distribution. The monitor at LCLS after the second bunch compressor with a nominal length of  $8\ \mu\text{m}$  at 250 pC is optimized with a  $30\ \mu\text{m}$  low pass filter. The calibration is done against absolute measurements using the transverse deflecting cavity. Fig. 6 shows the bunch length monitor signal as a function of the absolute bunch length [18] and a fit function obtained from the data which is used in the longitudinal feedback for LCLS.

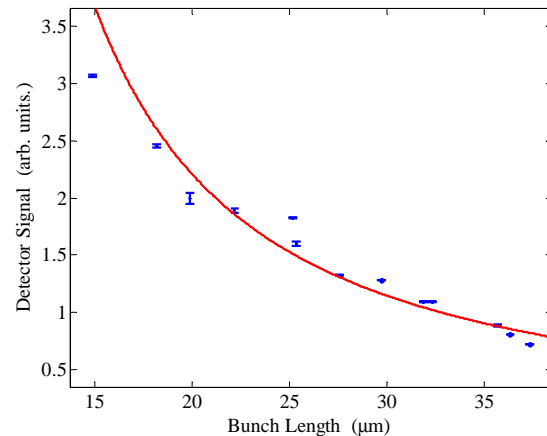


Figure 6: Calibration of the LCLS relative bunch length monitor signal to the absolute measurement with the transverse deflector.

More detailed information on the bunch structure in a relative bunch length monitor can be obtained by adding the capability of a single shot spectral measurement with a large number of channels over a wide wavelength range covering at least one decade. The grating bunch length monitor at FLASH has recently been converted into a single shot grating spectrometer [19] covering the spectral range from  $3\ \mu\text{m}$  to  $65\ \mu\text{m}$  with 6 different gratings and

20+ pyroelectric detector elements per grating. The spectral response of each channel is corrected for the transmission function of the radiation transport and the detector response, although an absolute calibration is difficult. Fig. 7 shows single shot spectra at normal on-crest (FEL) and off-crest operation. The micro-bunching structure in the near IR which is visible in both spectra has been subtracted from the normal operation spectrum to show the true bunch form factor. Fit curves obtained from a Gaussian and an asymmetric bunch shape agree well with the measured form factor.

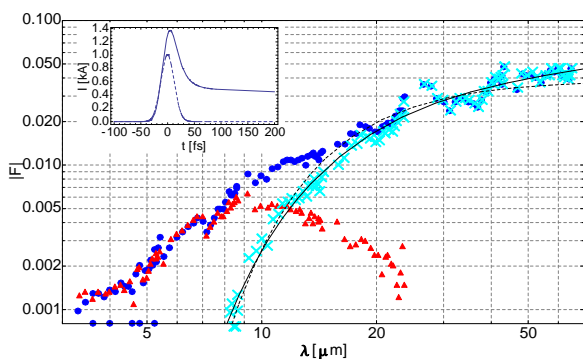


Figure 7: Single shot spectra of coherent transition radiation at FLASH from [19]. The blue dots represent the normal compressed, the red triangles the uncompressed operation showing microstructure in the near infrared, and the cyan crosses show the difference. The inset shows two fitted bunch profiles corresponding to the solid lines in the larger figure.

To be useful as an absolute single shot bunch length measurement, the calibration factors of the spectrometer need to be known with better accuracy. The application of this method can be extended into the visible and UV range to enable the measurement of sub-micron bunch lengths.

### Electro-Optic

Over the past decade, electro-optic detection schemes used in THz spectroscopy have been applied to directly measure the time distribution of the electric field of an electron bunch in a non-invasive way. These methods overcome the limitations of spectral intensity measurements for the phase reconstruction and the calibration of the transmission line.

In electro-optics detection the Coulomb field of a generated coherent radiation field of the beam travels through an electro-optic crystal and induces a transient birefringence in the crystal. A fs laser pulse is sent through the crystal and undergoes a phase retardation which is detected as an intensity change with a suitable arrangement of polarizers and wave plates.

A number of detection schemes have been developed in recent years and have been used at numerous accelerator

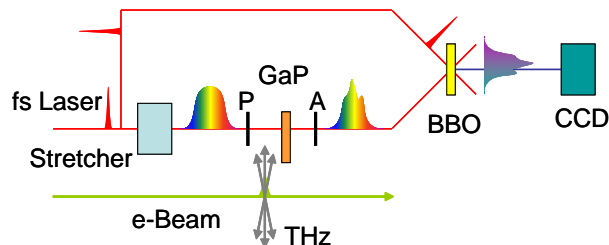


Figure 8: Schematic of the temporal encoding electro-optic detection scheme. The time distribution of the THz radiation pulse from the electron beam is encoded into the spectrum of a chirped fs laser pulse by detecting the induced phase retardation in the electro-optic crystal with polarizers. The time distribution of the encoded pulse can be retrieved by a cross-correlation with the original short laser pulse in a BBO crystal.

facilities. The scanning method where a variable delay between laser and electron beam samples the THz field [20] was converted to a single-shot measurement by encoding the THz time distribution into the spectrum of a chirped laser pulse [21] or into a spatial dimension [22]. More recently a resolution limitation of the spectral encoding was mitigated by directly measuring the time structure of the encoded pulse shape in the chirped laser pulse with a cross-correlation in a nonlinear crystal [23, 24]. Fig. 8 shows the principle of the detection scheme. The chirped pulse with the electron bunch shape temporally encoded is mixed in a BBO crystal with the original laser pulse in a non-collinear geometry. The sum frequency light contains spatially the pulse shape and is detected with a CCD.

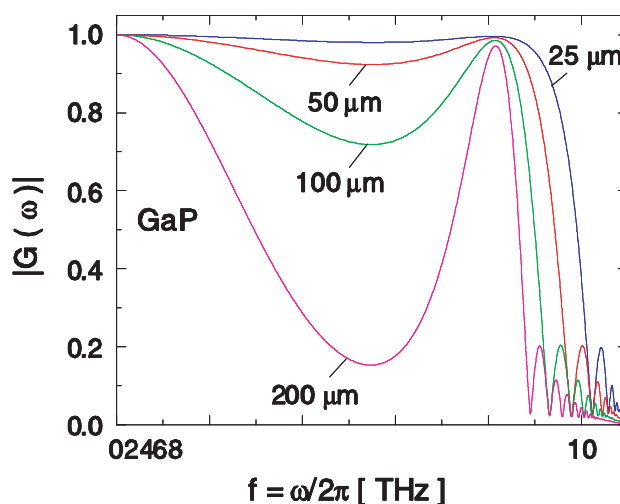


Figure 9: Geometric response function of GaP for electro-optic detection (from ([26])).

Different factors determine the temporal resolution of the method. The Coulomb field of the bunch at a distance  $b$  from the beam has a high frequency cut-off limiting the time resolution to  $b/\gamma c$  which is of the order of only a few



fs for a GeV beam with the crystal placed a few mm separated from the beam. The intrinsic pulse length of fs probe laser sets another limit to the time resolution, but can be some 10 fs. The most severe limitation presently is given by the response function of the electro-optic crystal. The phase retardation detected by the probe laser is the convolution of the Coulomb field with the response function [26] which takes into account both velocity and phase differences between laser and THz pulse and phonon absorption in the crystal. Figure 9 shows the geometric response function for GaP which to date is the most useful electro-optic material with the widest spectral bandwidth up to 10 THz or 30  $\mu\text{m}$ .

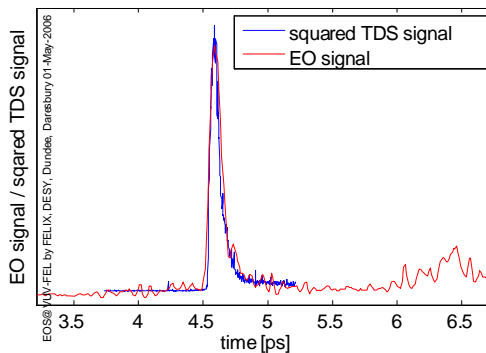


Figure 10: Comparison of the electro-optical temporal decoding technique with the transverse deflecting cavity measurement at FLASH (from [27]).

With this detection scheme bunch shapes with a peak rms length of 70 fs could be observed at FLASH and the bunch shape agrees well when compared to a transverse deflector cavity measurement [25]. Figure 10 shows both the bunch shape at the normal FEL mode obtained from a transverse deflector measurement and from the electro-optic method where a 65  $\mu\text{m}$  thick GaP crystal was used. The electro-optically measured pulse shape is slightly longer and smoother and the difference can be explained by a simulation taking the response function into account.

## SUMMARY

A wide range of diagnostics is nowadays available to measure the length of ps to sub-10fs long electron bunches from low energy up to 10s of GeV in an operationally convenient way as single-shot and non-invasive or minimally invasive techniques. The possibility of generating fs and sub-fs long bunches from high-brightness linear accelerators makes it necessary to extend existing techniques and to develop novel methods to make this regime accessible to bunch length diagnostics.

## ACKNOWLEDGEMENTS

The author wishes to thank all his coworkers in the LCLS commissioning team for their many contributions.

## REFERENCES

- [1] J. Arthur, *et al.*, Linac Coherent Light Source (LCLS) conceptual design report, SLAC-R-593, SLAC (2002).
- [2] SCSS X-FEL Conceptual Design Report, RIKEN (2005).
- [3] The European X-Ray Free-Electron Laser Technical Design Report, DESY 2006-097, DESY (2007).
- [4] E. R. Crosson, K. W. Berryman, B. A. Richman, T. I. Smith, R. L. Swent, Nucl. Instr. and Meth. A 375 (1996) 87.
- [5] H. Loos, *et al.*, Nucl. Instr. and Meth. A 528 (2004) 189.
- [6] O. H. Altenmueller, R. R. Larsen, G. A. Loew, Rev. Sci. Instrum. 35 (1964) 438.
- [7] M. Hüning, *et al.*, Proceedings of FEL 2005, Stanford, CA, Aug. 2005, p. 538 (2005).
- [8] R. Akre, *et al.*, Phys. Rev. ST Accel. Beams 11 (2008) 030703.
- [9] S. Molloy, *et al.*, Proceedings of PAC 2007, Albuquerque, NM, June 2007, p. FRPMS073 (2007).
- [10] K. Bane, *et al.*, Proceedings of FEL 2008, Gyeongju, Korea, Aug. 2008, p. TUPPH027 (2008).
- [11] Y. Ding, *et al.*, SLAC-PUB-13525, SLAC (2009).
- [12] A. Murokh, *et al.*, Proceedings of EPAC 2008, Genoa, Italy, June 2008, p. TUPC072 (2008).
- [13] H. Loos, *et al.*, Proceedings of FEL 2008, Gyeongju, Korea, Aug. 2008, p. THBAU01 (2008).
- [14] T. Nakazato, *et al.*, Phys. Rev. Lett. 63 (1989) 1245.
- [15] R. Lai, U. Happek, A. J. Sievers, Phys. Rev. E 50 (1994) R4294.
- [16] H. Delsim-Hashemi, *et al.*, Proceedings of EPAC 2006, Edinburgh, Scotland, June 2006, p. MOPCH016 (2006).
- [17] H. Loos, *et al.*, Proceedings of PAC 2007, Albuquerque, NM, June 2007, p. FRPMS071 (2007).
- [18] J. Wu, *et al.*, Proceedings of FEL 2008, Gyeongju, Korea, Aug. 2008, p. MOPPH052 (2008).
- [19] B. Schmidt, *et al.*, Proceedings of EPAC 2008, Genoa, Italy, June 2008, p. MOPC029 (2008).
- [20] X. Yan, *et al.*, Phys. Rev. Lett. 85 (2000) 3404.
- [21] I. Wilke, *et al.*, Phys. Rev. Lett. 88 (2002) 124801.
- [22] A. Cavalieri, *et al.*, Phys. Rev. Lett. 94 (2005) 114801.
- [23] S. P. Jamison, J. Shen, A. M. MacLeod, W. A. Gillespie, D. A. Jaroszynski, Opt. Lett. 28 (2003) 1710.
- [24] G. Berden, *et al.*, Phys. Rev. Lett. 93 (2004) 114802.
- [25] G. Berden, *et al.*, Phys. Rev. Lett. 99 (2007) 164801.
- [26] S. Casalbuoni, *et al.*, Phys. Rev. ST Accel. Beams 11 (2008) 072802.
- [27] P. J. Phillips, *et al.*, Proceedings of EPAC 2008, Genoa, Italy, June 2008, p. TUPC081 (2008).